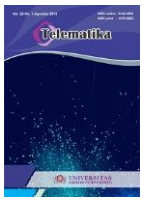

Available online at :
http://ejournal.amikompurwokerto.ac.id/index.php/telematika/

Telematika

Accreditated SINTA "2" Kemenristek/BRIN, No. 85/M/KPT/2020

UNIVERSITAS AMIKOM PURWOKERTO

Study of The Effect Stuart and Prandtl Numbers on Diamond Nano Fluid Flowing Through Cylindrical Surface

Yolanda Norasia[1], Mohamad Tafrikan[2], Mohammad Ghani[3], Asmianto[4], Indira Anggriani[5]

[1,2] Mathematic Department, Faculty Science and Technology,UIN Walisongo Semarang, Indonesia
[3.] Teknologi Sains Data, Fakultas Teknologi Maju dan Multidisiplin, Universitas Airlangga Surabaya, Indonesia
[4] Mathematic Department, Faculty of Math and Science, Universitas Negeri Malang, Indonesia
[5.]Mathematic Department, Institut Techonolgy Kalimantan, Indonesia
E-mail: yolandanorasia@walisongo.ac.id[1], tafrikan@walisongo.ac.id[2], mohammad.ghani@ftmm.unair.ac.id[3], asmianto.fmipa@um.ac.id[4], indira@lecturer.itk.ac.id [5]

ARTICLE INFO

History of the article:
Received August 15, 2022
Revised February 13, 2023
Accepted February 24, 2023

Keywords:
Diamond Nano Fluid
Stuart Number
Prandtl Number
CFD

Correspondece:
E-mail:
yolandanorasia@walisongo.ac.id

ABSTRACT

Fluid flow problems can be constructed using applied mathematical modeling and solved numerically using computational fluid dynamics (CFD). Nondimensional variables, stream functions, and similarity variables are used to simplify the governing equations from Newton's law, and thermodynamics law. These equations consist of continuity equations, momentum equations, and energy. Backward Euler method numerically solves the equations. The results show that the smaller the influence of the given Stuart number and Prandtl number, the fluid velocity and temperature will increase. Diamond nano fluid with water base fluid moves faster and experiences an increase in temperature faster than engine oil base fluid. this is due to the thermo-physical heat capacity of the water base fluid being greater than that of the engine oil.

INTRODUCTION

The study of fluid flow is an application of the field of computational fluid dynamics (CDF). Solution of fluid flow through a numerical approach using CDF. Fluids are divided into two categories, namely hydrostatic fluids and dynamic fluids. Fluids that have motion and can be observed are called hydrodynamic fluids. Turkyilmazoglu has carried out the control of hydrodynamic fluids using a magnetic field called magnetohydrodynamics (MHD). The research is about MHD fluid flow induced by a nonlinearly deforming permeable surface with mixed convection shows strong magnetic fields, and both momentum and temperature layers are thinned (Turkyilmazoglu, 2018). Kumar observed numerical solutions to the movement of MHD Cason Fluid numerically using Runge-Kutta. It is observed that radiation, temperature-dependent thermal conductivity, and irregular heat parameters influence velocity and temperature (Anantha et al., 2020). The Runge Kutta method is an explicitly numerical approach that has a maximum allowed limit in several time steps. The time step in these methods is generally quite small, especially for compressible flows (Hirsch, 2007).

Nanofluids are fluids with nanoparticle content ranging from one to one hundred nanometers. As nanofluids develop, they have become an important research area in physics, mathematics, engineering, and materials science. The use of nanofluids to enhance thermal diffusive, thermally conductive, and

convective heat transfer has increasingly become common in industrial applications. Nanofluids can increase energy efficiency so this research is interesting to be developed further. Fluid flow containing Titania, Copper, and Alumina nanoparticles by micro-rotation through circular cylinders was carried out by (Abbas et al., 2018). The research used a numerical solution using the Runge-Kutta scheme. The results show the maximum heat transfer rate for Copper compared to Titania and Alumina (Abbas et al., 2018). Research about increasing the concentration of nanofluids can reduce the maximum fluid velocity (Ghalandari et al., 2019). The heat rate in the nanofluid increases with the addition of the MHD parameter has been investigated (Nadeem et al., 2020a). Research on nanofluid flow under magnetic effects shows that fluid movement slows down with increasing magnetic variation (Norasia et al., 2021). By enhancing Brownian motion and thermophoresis parameters, the nanofluid flow through the two parallel disks increases significantly in terms of energy profiles (Alotaibi, 2022). The movement of fluids is affected by nondimensional parameters, which are crucial for analyzing fluid behavior. The Prandtl number is one of the nondimensional parameters used to observe the behavior of the diffusivity of momentum with temperature (Reddy et al., 2018). Particles interacting with each other produce momentum and heat energy through friction. The effect of the Prandtl number can affect the thermal characteristics of the fluid (Yu et al., 2020). Another nondimensional parameter is the Stuart number, which is a number that observes fluid behavior through electromagnetic and surface forces (Lee et al., 2005). Studies on the effects of electromagnetic forces on nanofluid flow show that they can lead to an increase in shear stress (Shahzad et al., 2022).

Referring to the results of previous research, nanofluids are interesting for further research. Diamond nano fluid is a fluid that can improve thermal performance. Research on the application of diamond nanofluid in heat pipes can extract heat flux so that diamond nanofluid can be used as a cooling device (Ma et al., 2006). Engine oil containing nanodiamond particles shows an increase in thermal conductivity and specific heat (Ghazvini et al., 2012). In comparison to other metal oxide nanoparticles, diamond nanofluid exhibits better thermal conductivity of 1000WmK (Aun et al., 2017). Diamond fluid flow characteristics such as velocity and temperature are interesting for future research. This study using diamond nanofluid which means a mixture of diamond nanoparticles and base fluid. Variations of the basic fluids used are water and engine oil.The existence of flow control using magnetic and thermal performance, this research involves the influence of Stuart number and Prandtl number. This study aims to examine the velocity and temperature of the diamond nanofluid by involving the Stuart number and Prandtl number that pass through cylindrical surface which is solved numerically using the Backward Euler method. This method is used to calculate a fairly high level of stability (Hirsch, 2007) (Freziger & Peric, 2002). It allows arbitrarily large time steps to be taken, which makes it useful for studying slow transient flows (Freziger & Peric, 2002). Not much has been done to apply the Backward Euler method to fluid flow models. Therefore, we are interested in applying the method to model the flow of diamond nanofluid pass through cylindrical surface.

RESEARCH METHODS

The purpose of this section is to describe the materials used for the research as well as the equipment used for the method. The steps to solve the problem are also explained.

1. Mathematical modeling

In this step, the governing equations are used as a mathematical model of diamond nano fluid flow through cylindrical surface. The steps of model development are given as follows.

a. A three-dimensional equation of continuity, momentum, and energy is formed by governing equations based on laws of physics.
b. The obtained dimensional equations are converted into nondimensional equations by using nondimensional variables and nondimensional parameters.
c. The obtained nondimensional equations are substituted using the thermo-physical variable of the diamond nano fluid.
d. Simplification of the obtained nondimensional equations into one variable for ease of computation using flow functions and similarity variables.

2. Numerical solution

The numerical solution of the mathematical model of the diamond nano fluid flow obtained is completed through the numerical approach of the Backward Euler method.The implicit schema approach uses the following steps.

a. The similarity equation in momentum and energy is solved by implicit scheme.
b. Identify the coefficients and constants of the tridiagonal matrix obtained.
c. Applying Thomas's algorithm through forward elimination and backward substitution for solving the tridiagonal matrix.

3. Results analysis and discussion

On this step, an analysis of the results of the influence of related parameters, namely the Stuart number and Prandtl number, are carried out on the flow of diamond nano fluid passing through cylindrical surface.

Mathematical Modeling

The basic equations derived from the laws of physics given as follows. Equation of continuity based on conservation of mass law (Chung, 2010) : $\frac{DM_f}{Dt} = 0$, Equation of momentum based on Newton's second law (Sheikholeslami & Rokni, 2017): $\rho_f \frac{DV}{Dt} = -\nabla \boldsymbol{p} + \rho_f \upsilon \nabla^2 u + \sum F$, Equation of energy based on Thermodynamics law (Chung, 2010):$\rho_f \frac{De}{Dt} = \rho_f \frac{\partial e}{\partial t} + \rho_f \boldsymbol{V}.\nabla \boldsymbol{e}$.

In this study, the dimensional governing equation in unsteady and incompressible according to the laws of physics conditions as follows:

Equation of dimensional-continuity

$$\frac{\partial \bar{u}}{\partial \bar{x}} + \frac{\partial \bar{v}}{\partial \bar{y}} = 0, \quad (1)$$

Equation of dimensional-momentum

on the *x*-axis

$$\rho_{f_{DN}} \left(\frac{\partial \bar{u}}{\partial \bar{t}} + \bar{u}\frac{\partial \bar{u}}{\partial \bar{x}} + \bar{v}\frac{\partial \bar{u}}{\partial \bar{y}}\right) = -\nabla p + \mu_{f_{DN}} \nabla^2 \mathbf{V} + \left(\rho_{f_{DN}} - \rho_\infty\right) g_{\bar{x}} + \sigma(\mathrm{B}_0)^2 \bar{u}, \quad (2)$$

on the *y*-axis

$$\rho_{f_{DN}} \left(\frac{\partial \bar{v}}{\partial \bar{t}} + \bar{u}\frac{\partial \bar{v}}{\partial \bar{x}} + \bar{v}\frac{\partial \bar{v}}{\partial \bar{y}}\right) = -\nabla p + \mu_{f_{DN}} \nabla^2 \mathbf{V} + \left(\rho_{f_{DN}} - \rho_\infty\right) g_{\bar{y}} + \sigma(\mathrm{B}_0)^2 \bar{v}, \quad (3)$$

Equation of dimensional-energy

$$\left(\frac{\partial \bar{T}}{\partial \bar{t}} + \bar{u}\frac{\partial \bar{T}}{\partial \bar{x}} + \bar{v}\frac{\partial \bar{T}}{\partial \bar{y}}\right) = \alpha_{f_{DN}} \left(\frac{\partial^2 \bar{T}}{\partial \bar{x}^2} + \frac{\partial^2 \bar{T}}{\partial \bar{y}^2}\right). \quad (4)$$

the boundary condition given as follows.

$\bar{u} = \bar{v} = 0, \bar{T} = T_w$,when $\bar{y} = 0$

$\bar{u} = \bar{u}_e$,$T = T_\infty$ when $\bar{y} \to \infty$.

Dimensional equations (1)-(4) are converted into nondimensional equations by using nondimensional variables and nondimensional parameters as follows.

Nondimensional variables defined as follow (Azam et al., 2020).

$$x = \frac{\bar{x}}{a}; y = \left(\frac{u_\infty a}{v_f}\right)^{1/2} \frac{\bar{y}}{a}; t = \frac{U_\infty \bar{t}}{a}; u = \frac{\bar{u}}{U_\infty}; v = \left(\frac{u_\infty a}{v_f}\right)^{1/2} \frac{\bar{v}}{U_\infty}$$

$$T = \frac{\bar{T} - T_\infty}{T_w - T_\infty}; \; P = \frac{\bar{P}}{\rho_{f_{DN}} {U_\infty}^2}; u_e(x) = \frac{\bar{u}_e(\bar{x})}{v_\infty}$$

Nondimensional parameters defined as follow (Korotaeva et al., 2020), (Amanulla et al., 2019).

$$St = \frac{\sigma B_0 a}{U_\infty \rho} \text{ and } Pr = \frac{\nu}{\alpha}$$

then, we get

Equation of nondimensional-continuity

$$\frac{\partial u}{\partial x} + \frac{\partial v}{\partial y} = 0, \tag{5}$$

Equation of nondimensional-momentum

on the *x*-axis

$$\frac{\partial u}{\partial t} + u\frac{\partial u}{\partial x} + v\frac{\partial u}{\partial y} = -\frac{\partial p}{\partial x} + \frac{v_{f_{DN}}}{Re\, v_B}\frac{\partial^2 u}{\partial x^2} + \frac{v_{f_{DN}}}{v_B}\frac{\partial^2 u}{\partial y^2} + St\, u + \lambda T sin\, x, \tag{6}$$

on the *y*-axis

$$\frac{1}{Re}\left(\frac{\partial v}{\partial t} + u\frac{\partial v}{\partial x} + v\frac{\partial v}{\partial y}\right) = -\frac{\partial p}{\partial x} + \frac{v_{f_{DN}}}{v_B}\frac{1}{Re^2}\frac{\partial^2 v}{\partial x^2} + \frac{v_{f_{DN}}}{v_B}\frac{1}{Re}\frac{\partial^2 v}{\partial y^2} + \frac{St}{Re}v - \frac{\lambda}{Re^{0.5}} T cos\, x, \tag{7}$$

Nondimensional-energy equation

$$\frac{\partial T}{\partial t} + u\frac{\partial T}{\partial x} + v\frac{\partial T}{\partial y} = \frac{1}{Re}\frac{1}{Pr}\frac{\alpha_{f_{DN}}}{\alpha_B}\frac{\partial^2 T}{\partial x^2} + \frac{1}{Pr}\frac{\alpha_{f_{DN}}}{\alpha_B}\frac{\partial^2 T}{\partial y^2}. \tag{8}$$

Thermo-physical diamond nano fluid variables are defined as follows (Norasia et al., 2021) (Huda et al., 2017).

$$\rho_{f_{DN}} = (1-\chi)\rho_B + \chi\rho_D\,, \mu_{f_{DN}} = \frac{\mu_B e^{-\alpha T}}{(1-\chi)^{2.5}},$$

$$(\rho C_p)_{f_{DN}} = (1-\chi)(\rho C_p)_B + \chi(\rho C_p)_D, \; k_{f_{DN}} = k_B\left(\frac{k_D + 2k_B - 2\chi(k_D - k_B)}{k_D + 2k_B + \chi(k_D - k_B)}\right).$$

by substituting the thermo-physical diamond nano fluid variables, then equations (5)-(8) become as follows.

Nondimensional-continuity equation

$$\frac{\partial u}{\partial x} + \frac{\partial v}{\partial y} = 0, \tag{9}$$

Equation of nondimensional-momentum

on the *x*-axis

$$\frac{\partial u}{\partial t} + u\frac{\partial u}{\partial x} + v\frac{\partial u}{\partial y} = -\frac{\partial P}{\partial x} + \left(\frac{1}{(1-\chi)^{2.5}}\frac{1}{(1-\chi)+\chi\left(\frac{\rho_D}{\rho_B}\right)}\right)\frac{\partial^2 u}{\partial y^2} + St\, u + \lambda T sin\, x, \tag{10}$$

on the *y*-axis

$$\frac{\partial p}{\partial y} = 0, \tag{11}$$

Nondimensional-energy equation

$$\left(\frac{\partial T}{\partial t}+u\frac{\partial T}{\partial x}+v\frac{\partial T}{\partial y}\right)=\frac{1}{Pr}\frac{k_D+2k_B-2\chi(k_D-k_B)}{k_D+2k_B+\chi(k_D-k_B)}\frac{1}{(1-\chi)+\chi\left(\frac{(\rho C_p)_D}{(\rho C_p)_B}\right)}\frac{\partial^2 T}{\partial y^2}. \quad (12)$$

Then, the obtained nondimensional equation is simplified using the stream function and the similarity variables which are defined sequentially as follows (Nadeem et al., 2022b).

$u=\frac{\partial \psi}{\partial y}$; $v=-\frac{\partial \psi}{\partial x}$; and $\Psi=t^{\frac{1}{2}}u_e(x)f(x,\eta,t)$; $\eta=\frac{y}{t^{1/2}}$; $T=s(x,\eta,t)$

Equations (9)-(12) become as follows.

Similarity-momentum equation

$$M\frac{\partial^3 f}{\partial \eta^3}+\frac{\eta\partial^2 f}{2\partial\eta^2}+t\frac{\partial u_e}{\partial x}\left[1-\left(\frac{\partial f}{\partial \eta}\right)^2+f\frac{\partial^2 f}{\partial \eta^2})\right]=t\frac{\partial^2 f}{\partial\eta\partial t}+tu_e\left(\frac{\partial f}{\partial\eta}\frac{\partial^2 f}{\partial x\partial\eta}-\frac{\partial f}{\partial x}\frac{\partial^2 f}{\partial\eta^2}-f\frac{\partial^2 f}{\partial\eta^2}\right)+St\ t\left(1-\frac{\partial f}{\partial\eta}\right)-\frac{\lambda st}{u_e}\sin x, \quad (13)$$

Similarity-energy equation

$$N\frac{\partial^2 s}{\partial\eta^2}+Pr\frac{\eta}{2}\frac{\partial s}{\partial\eta}+Pr\ t\frac{\partial u_e}{\partial x}f\frac{\partial s}{\partial\eta}=Pr\ t\left[\frac{\partial s}{\partial\eta}+u_e\left(\frac{\partial f}{\partial\eta}\frac{\partial s}{\partial x}-\frac{\partial f}{\partial x}\frac{\partial s}{\partial\eta}-f\frac{\partial s}{\partial\eta}\right)\right]. \quad (14)$$

with $M=\left[\frac{1}{(1-\chi)^{2.5}\left[(1-\chi)+\chi\left(\frac{\rho_D}{\rho_B}\right)\right]}\right]$ and $N=\left(\frac{k_D+2k_B-2\chi(k_D-k_B)}{k_D+2k_B+\chi(k_D-k_B)}M\right)$.

the boundary condition given as follows.

$f=\frac{\partial f}{\partial\eta}=0, T=1$ when $y=0$

$\frac{\partial f}{\partial y}=1, T=0$ when $y\to\infty$.

the application of the Backward Euler method to Equation (13) is obtained.

$$\frac{M}{\Delta\eta^2}\left(u_{i+1}^{k+1}-2u_i^{k+1}+u_{i-1}^{k+1}\right)+\frac{\eta_i}{4}\left(\frac{3u_{i+1}^{k+1}-4u_i^{k+1}+u_{i-1}^{k+1}}{\Delta\eta}\right)+\frac{3}{2}t^{k+1}\left(1-\left(u_i^{k+1}\right)^2+\frac{f_i^k}{\Delta\eta}\left(3u_{i+1}^{k+1}-4u_i^{k+1}+u_{i-1}^{k+1}\right)\right)=\frac{t^{k+1}}{2\Delta t}\left(3u_i^{k+1}-4u_i^{k+1}+u_i^{k+1}\right)+St\ t^{k+1}\left(1-u_i^{k+1}\right)-\lambda s_i^k t^{k+1},$$

The discretization of the momentum equation is given as follows.

$-(C_1)\Delta u_{i-1}^{k+1}+(C_2)\Delta u_{i-1}^{k+1}-(C_3)\Delta u_{i-1}^{k+1}=Ci$,with

$$C_i=\frac{M}{\Delta\eta^2}\left(u_{i+1}^{k+1}-2u_i^{k+1}+u_{i-1}^{k+1}\right)+\frac{\eta_i}{4}\left(\frac{3u_{i+1}^{k+1}-4u_i^{k+1}+u_{i-1}^{k+1}}{\Delta\eta}\right)+\frac{3}{2}t^{k+1}\left(1-\left(u_i^{k+1}\right)^2+\frac{f_i^k}{\Delta\eta}\left(3u_{i+1}^{k+1}-4u_i^{k+1}+u_{i-1}^{k+1}\right)\right)-St\ t^{k+1}\left(1-u_i^{k+1}\right)+\lambda s_i^k t^{k+1}$$,then

$$C_1=\frac{M}{\Delta\eta^2}+\frac{\eta_i}{4}\frac{1}{\Delta\eta}+\frac{3}{2}t^{k+1}\frac{f_i^k}{\Delta\eta},$$

$$C_2=\frac{3}{2}\frac{t^{k+1}}{\Delta t}+2\frac{M}{\Delta\eta^2}-St\ t^{k+1}+3t^{k+1}u_i^k+\frac{\eta_i}{\Delta\eta}+6\ t^{k+1}\frac{f_i^k}{\Delta\eta},$$

$$C_3=\frac{M}{\Delta\eta^2}+\frac{3}{4}\eta_i\frac{1}{\Delta\eta}+\frac{9}{2}t^{k+1}\frac{f_i^k}{\Delta\eta}.$$

the application of the Backward Euler method to Equation (14) is obtained.

$$\frac{N}{\Delta\eta^2}\left(s_{i+1}^{k+1}-2s_i^{k+1}+s_{i-1}^{k+1}\right)+Pr\frac{\eta_i}{2}\left(\frac{3s_{i+1}^{k+1}-4s_i^{k+1}+s_{i-1}^{k+1}}{\Delta\eta}\right)+\frac{3}{2}Pr\ t^{k+1}\frac{f_i^k}{2\Delta\eta}\left(3s_{i+1}^{k+1}-4s_i^{k+1}+s_{i-1}^{k+1}\right)=\frac{1}{2}Pr\frac{t^{k+1}}{\Delta t}\left(3s_{i+1}^{k+1}-4s_i^{k+1}+s_{i-1}^{k+1}\right),$$

The discretization of the momentum equation is given as follows.

$-(D_1)\Delta s_{i-1}^{k+1}+(D_2)\Delta s_{i-1}^{k+1}-(D_3)\Delta s_{i-1}^{k+1}=Di$, with

$D_i = \frac{N}{\Delta\eta^2}\left(s_{i+1}^{k+1} - 2s_i^{k+1} + s_{i-1}^{k+1}\right) + Pr\frac{\eta_i}{2}\frac{1}{\Delta\eta}\left(3s_{i+1}^{k+1} - 4s_i^{k+1} + s_{i-1}^{k+1}\right) + 3Pr\, t^{k+1}\frac{f_i^k}{2\Delta\eta}\left(3s_{i+1}^{k+1} - 4s_i^{k+1} + s_{i-1}^{k+1}\right)$, then

$D_1 = \frac{N}{\Delta\eta^2} + \frac{\eta_i}{4}\frac{1}{\Delta\eta}Pr + \frac{3}{2}t^{k+1}\frac{f_i^k}{\Delta\eta}Pr,$

$D_2 = \frac{3}{2}t^{k+1}\frac{1}{\Delta t}Pr + 2\frac{N}{\Delta\eta^2} + \eta_i\frac{1}{\Delta\eta}Pr + 6\, t^{k+1}\frac{f_i^k}{\Delta\eta}Pr\,,$

$D_3 = \frac{M}{\Delta\eta^2} + \frac{3}{4}\,\eta_i\frac{1}{\Delta\eta}Pr + \frac{9}{2}t^{k+1}\frac{f_i^k}{\Delta\eta}Pr.$

RESULTS AND DISCUSSION

The similarity equation obtained is solved using the numerical solution of the Backward Euler Method. The fluid used in this study is diamond nano fluid. Diamond nano fluid is a fluid with diamond nano particles and a base fluid. The base fluids used in this research are water and engine oil. The following is for the thermo-physical of diamond nanoparticles and the base fluid (Adnan et al., 2022).

Table 1. Thermo-Physical of Diamond nano Fluid

Thermo-physical	$\rho(kg/m^3)$	$c_p\left(\frac{J}{kg\ K}\right)$	$k\left(\frac{W}{mK}\right)$
Diamond	3100	516	1000
Water	997.1	4179	0.613
Engine oil	884	1910	0.144

The velocity and temperature rate of the diamond nano fluid flow with the water base fluid are shown in Figure 1 and Figure 2. The base fluid used is water so for the input constant values for the Prandtl number, convection, and volume fraction respectively are $Pr = 13, \lambda = 1, \chi = 0.1$. Meanwhile, the input to the Stuart number is variance $St = 0,3,10,15,20$.

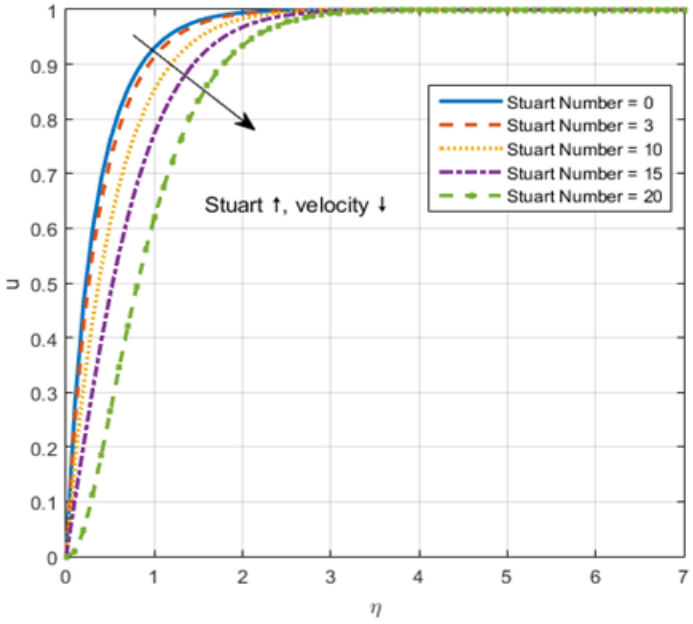

Figure 1. Variation of Stuart numbers on nano diamond-water fluid temperature

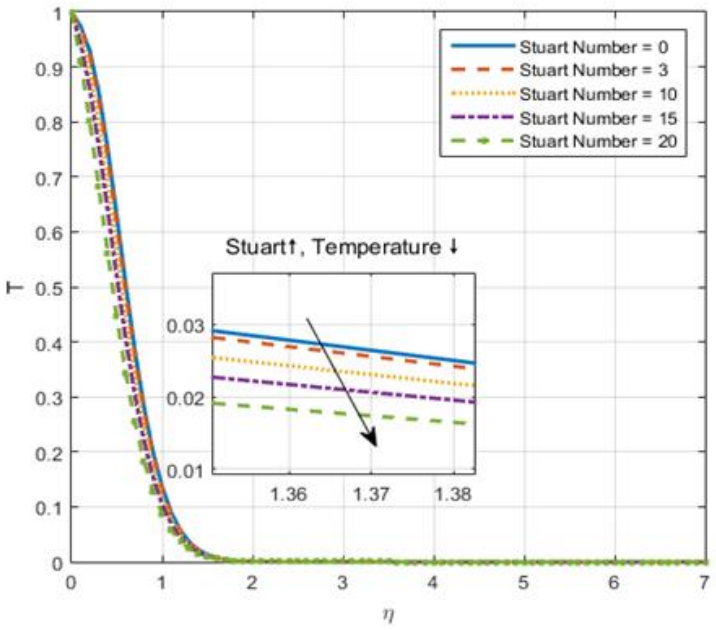

Figure 2. Variation of Stuart numbers on diamond nano-water fluid velocity

The Stuart number parameter ranges from 0 to 20, where the Stuart number starts from 0 and increases in variance up to 20. In the case of nano-diamond-water, $St = 0$ means the Stuart number has not had any impact on the fluid. Figure 1 shows that the velocity of the diamond nano-water fluid decreases with the increase in the variation of the Stuart number. This is due to the influence of a magnet that causes a resistance force in the form of the Lorentz Force. The diamond nano-water fluid's velocity decreases as the Stuart number parameter increases. The existence of the Lorentz Force also causes a decrease in the fluid temperature as shown in Figure 2.

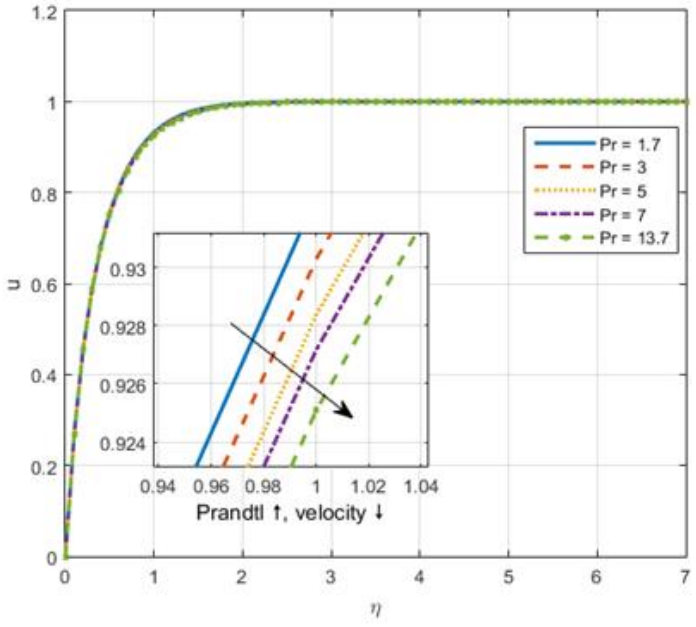

Figure 3. Variation of Prandtl numbers on nano diamond-water fluid velocity

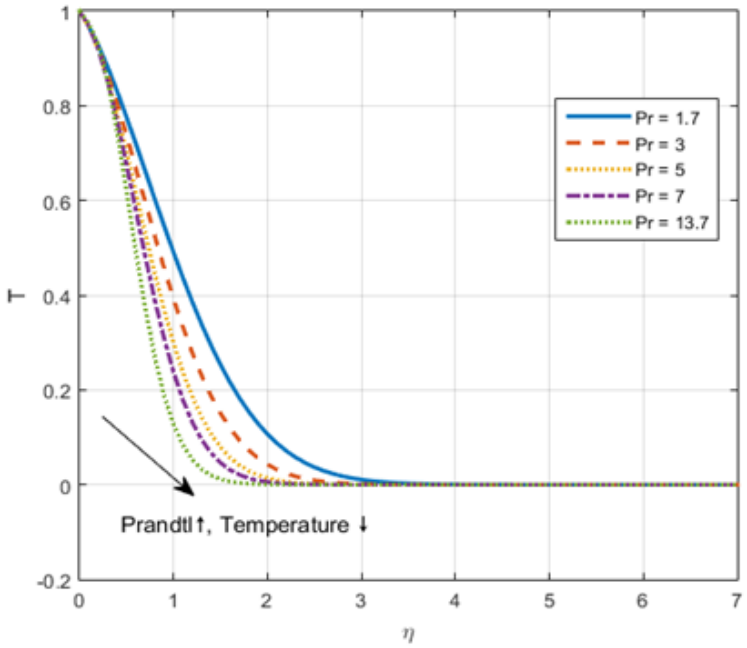

Figure 4. Variation of Prandtl numbers on nano diamond-water fluid temperature

The velocity and temperature rate of the diamond nano-water fluid flow with Prandtl number variation are shown in Figure 3 and Figure 4. The input constant values for the Stuart number, convection, and volume fraction respectively are $St = 1, \lambda = 1, \chi = 0.1$. The range of Prandtl numbers in water-based fluids is 1.7 to 13.7 so that the variance of the Prandtl numbers used are $Pr = 1.7, 3, 5, 7, 13.7$. In Figure 3 and Figure 4 it can be seen that the diamond nanoparticles with the highest Prandtl number experience a decrease in fluid velocity and temperature. Viscous effects are stronger with a higher Prandtl Number variance than with a higher thermal diffusivity. Consequently, a larger Prandtl number makes diamond-water nanofluids less stable.

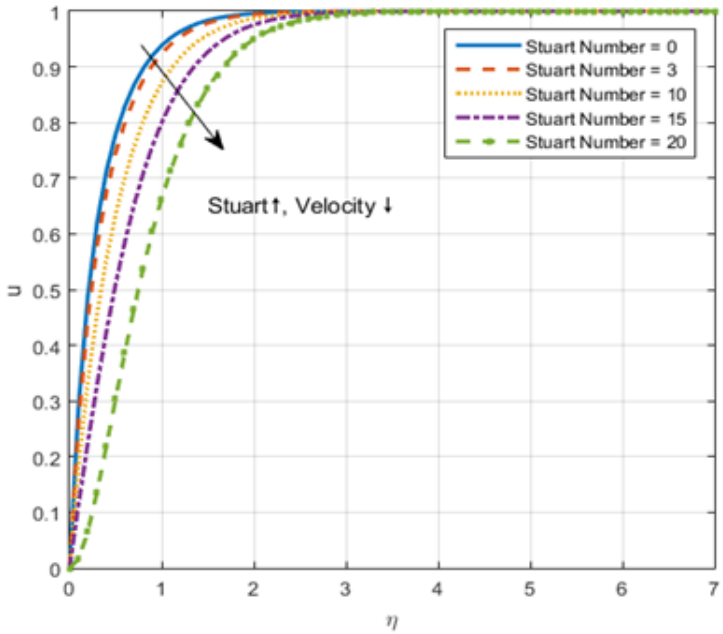

Figure 5. Variation of Stuart numbers on nano

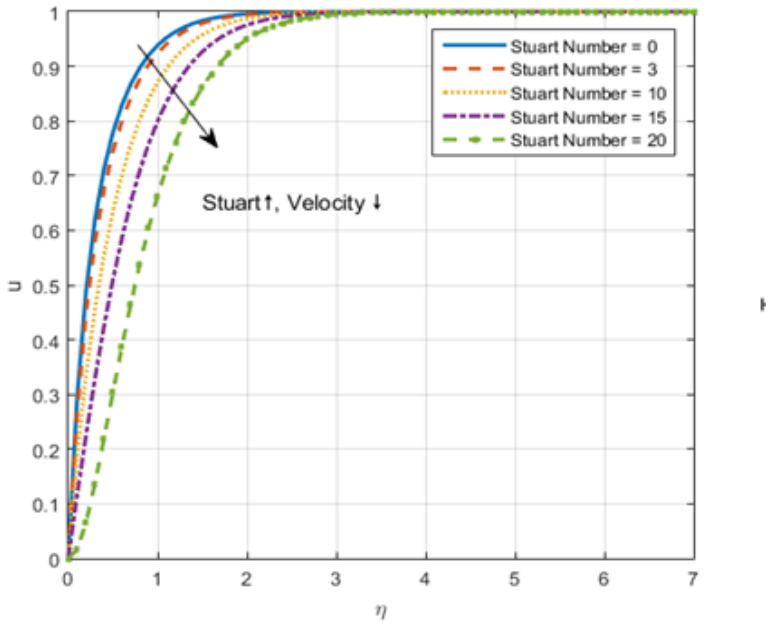

Figure 5. Variation of Stuart numbers on nano nano-engine oil fluid velocity

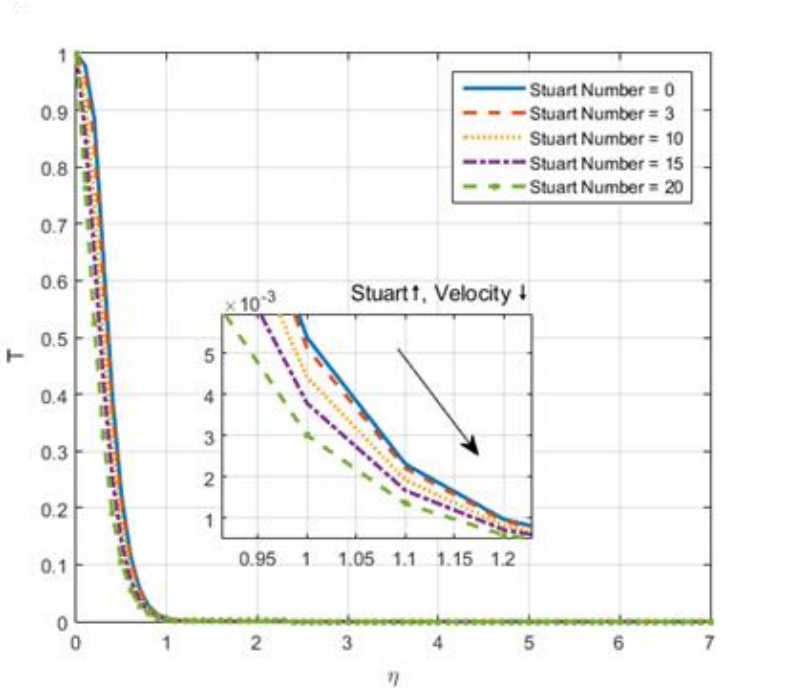

Figure 6. Variation of Stuart numbers on diamond diamond-engine oil fluid temperature

The velocity and temperature rate of the diamond nano fluid flow with the engine oil base fluid are shown in Figure 5 and Figure 6. The base fluid used is water so for the input constant values for the Prandtl number, convection, and volume fraction respectively are $Pr = 50, \lambda = 1, \chi = 0.1$. Meanwhile, the input to the Stuart number is variance $St = 0, 3, 10, 15, 20$. In Figure 5, the fluid velocity of diamond nano-engine oil decreases as the Stuart number parameter increases. The Lorentz force affects the engine oil base fluid and diamond nanoparticles, causing a reduction in velocity. Figure 6 shows that the fluid temperature also decreases as the Stuart number parameter increases. It occurs because of the relationship between

Stuart parameters and fluid internal energy. Temperatures of fluids decrease with greater internal energy use.

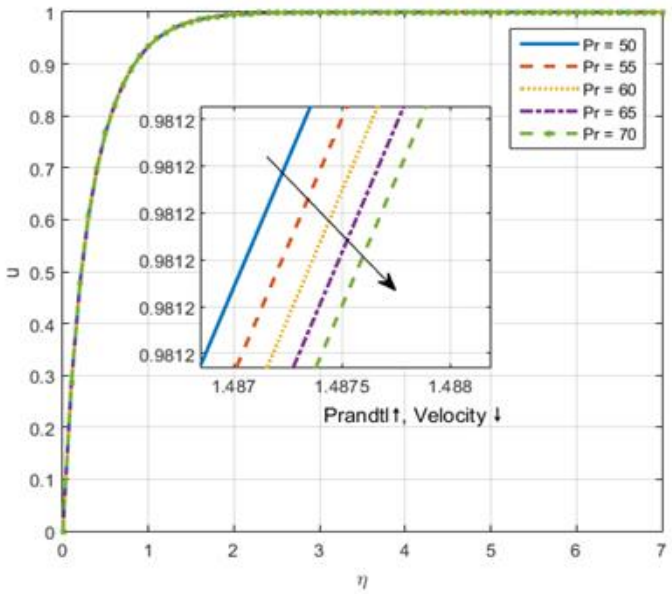

Figure 7. Variation of Prandtl numbers on nano diamond-engine oil fluid velocity

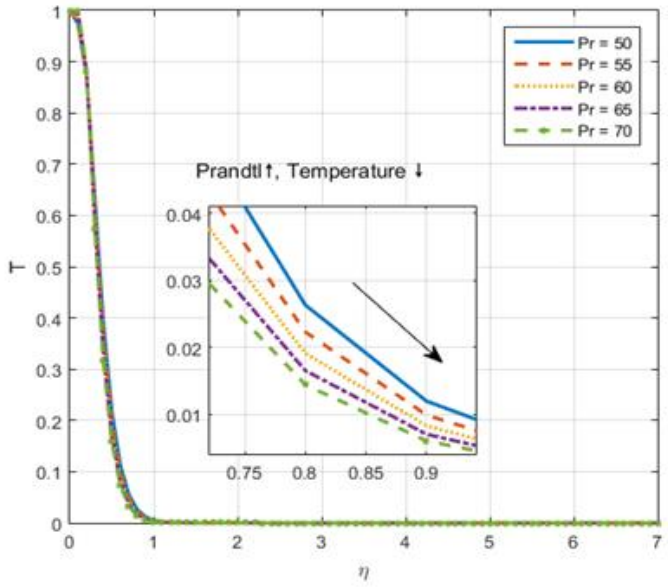

Figure 8. Variation of Prandtl numbers on nano diamond-engine oil fluid velocity

The velocity and temperature rate of the diamond nano-engine oil fluid flow with Prandtl number variation are shown in Figure 7 and Figure 8. The input constant values for the Stuart number, convection, and volume fraction respectively are $St = 1, \lambda = 1, \chi = 0.1$. The range of Prandtl numbers in water-based fluids is 50 to 70 so that the variance of the Prandtl numbers used are $Pr = 50,55,60,65,70$. Figure 7 shows that the fluid flow velocity increases when the Prandtl number decreases. Since the Prandtl number increases directly with kinematic viscosity, fluid density increases along with the Prandtl number, so velocity decreases as the Prandtl number increases. Increasing the Prandtl number parameter causes the temperature to decrease because it is inversely related to thermal diffusivity.

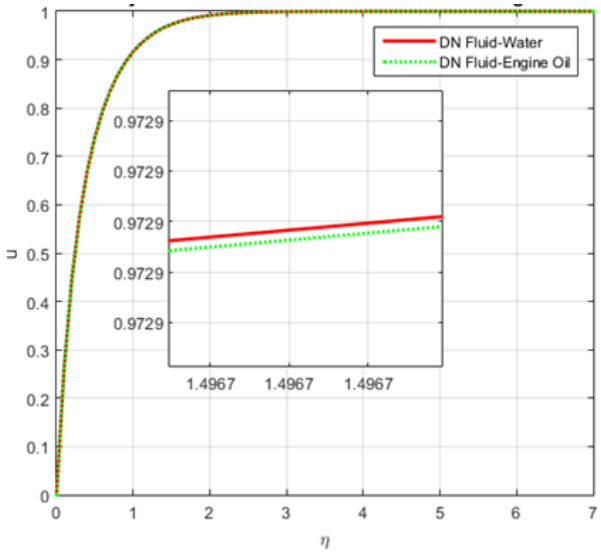

Figure 9. Velocity rate of diamond nano-water fluid and diamond nano-engine oil fluid

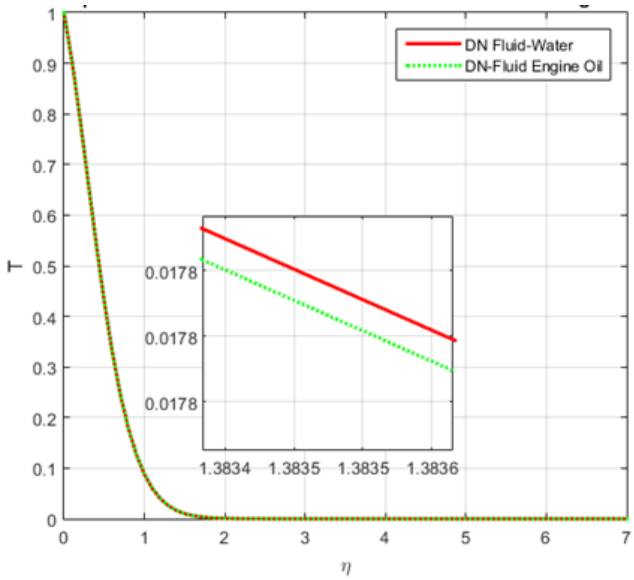

Figure 10. Temperature rate of diamond nano-water fluid and diamond nano-engine oil fluid

The velocity of the diamond nano-water fluid and the diamond nano-engine oil fluid are shown in Figure 9 and Figure 10. The input constant values for the Stuart number, Prandtl number, convection, and volume fraction respectively are $St = 1, Pr = 2\,\lambda = 1, \chi = 0.01$. Figure 9 shows that the diamond nano-water fluid is faster than the diamond nano-engine oil fluid. Then, Figure 10 shows that the diamond nano-water fluid experiences an increase in temperature faster than the diamond nano-engine oil fluid. This happens because the heat capacity of the water base fluid ($C_p = 4179$) is greater than that of the engine oil ($C_p = 1910$). As the heat capacity increases, the temperature rises. Diamond particles in diamond nano-water move faster when the fluid temperature rises. As a result, the fluid velocity in the diamond nano-water fluid increases faster than in the diamond nano-engine oil fluid.

CONCLUSIONS AND RECOMMENDATIONS

A study the effect of the Stuart and Prandtl numbers on diamond nano fluid flowing through cylindrical surface has been observed. Mathematical modeling of diamond nanofluid flow is built from the

Continuity Equation, momentum equation, and energy equation. The solution is done through a numerical approach using the Backward Euler Method. The results show that the smaller the influence of the given Stuart number and Prandtl number, the fluid velocity and temperature will increase. Diamond nano fluid with water base fluid moves faster and experiences an increase in temperature faster than engine oil base fluid. this is due to the thermo-physical heat capacity of the water base fluid being greater than that of the engine oil.

REFERENCES

Abbas, N., Saleem, S., Nadeem, S., Alderremy, A. A., & Khan, A. U. (2018). On stagnation point flow of a micro polar nanofluid past a circular cylinder with velocity and thermal slip. *Results in Physics*, *9*(January), 1224–1232. https://doi.org/10.1016/j.rinp.2018.04.017

Adnan, K, U., Ahmed, N., Mohyud-Din, S. T., Alsulami, M. D., & Khan, I. (2022). A novel analysis of heat transfer in the nanofluid composed by nanodimaond and silver nanomaterials: numerical investigation. *Scientific Reports*, *12*(1), 1–11. https://doi.org/10.1038/s41598-021-04658-x

Alotaibi, H. (2022). *Numerical simulation of nano fl uid fl ow between two parallel disks using 3 - stage Lobatto III - A formula*. 649–656.

Amanulla, C. H., Saleem, S., Wakif, A., & Alqarni, M. M. (2019). MHD Prandtl fluid flow past an isothermal permeable sphere with slip effects. *Case Studies in Thermal Engineering*, *14*(April). https://doi.org/10.1016/j.csite.2019.100447

Anantha K, K., Sugunamma, V., & Sandeep, N. (2020). Effect of thermal radiation on MHD Casson fluid flow over an exponentially stretching curved sheet. *Journal of Thermal Analysis and Calorimetry*, *140*(5), 2377–2385. https://doi.org/10.1007/s10973-019-08977-0

Aun, T. S., Abdullah, M. Z., & Gunnasegaran, P. (2017). Influence of low concentration of diamond water nanofluid in loop heat pipe. *International Journal of Heat and Technology*, *35*(3), 539–548. https://doi.org/10.18280/ijht.350310

Azam, M., Xu, T., & Khan, M. (2020). Numerical simulation for variable thermal properties and heat source/sink in flow of Cross nanofluid over a moving cylinder. *International Communications in Heat and Mass Transfer*, *118*. https://doi.org/10.1016/j.icheatmasstransfer.2020.104832

Chung, T. J. (2010). Computational fluid dynamics, second edition. In *Computational Fluid Dynamics, Second Edition* (Vol. 9780521769). https://doi.org/10.1017/CBO9780511780066

Freziger, J. H., & Peric, M. (2002). *Computational Methods for Fluid Dynamics* (3rd ed.). Spinger.

Ghalandari, M., Koohshahi, E. M., Shamshirband, S., & Chau, K. W. (2019). *Mechanics Numerical simulation of nanofluid flow inside a root canal*. *2060*. https://doi.org/10.1080/19942060.2019.1578696

Ghazvini, M., Akhavan-Behabadi, M. A., Rasouli, E., & Raisee, M. (2012). Heat transfer properties of nanodiamond-engine oil nanofluid in laminar flow. *Heat Transfer Engineering*, *33*(6), 525–532. https://doi.org/10.1080/01457632.2012.624858

Hirsch, C. (2007). *Numerical Computation of Internal and External Flows*. John Wiley & Sons. https://doi.org/10.2514/5.9781600868245.0357.0409

Huda, A. B., Akbar, N. S., Beg, O. A., & Khan, M. Y. (2017). Dynamics of variable-viscosity nanofluid flow with heat transfer in a flexible vertical tube under propagating waves. *Results in Physics*, *7*(January), 413–425. https://doi.org/10.1016/j.rinp.2016.12.036

Korotaeva, T. A., Fomichev, V. P., & Yadrenkin, M. A. (2020). Numerical and Experimental Simulation of Magnetohydrodynamic Interaction in a Hypersonic Flow of a Blunt Body. *Journal of Applied Mechanics and Technical Physics*, *61*(2), 162–170. https://doi.org/10.1134/S0021894420020029

Lee, H. G., Ha, M. Y., & Yoon, H. S. (2005). A numerical study on the fluid flow and heat transfer in the confined jet flow in the presence of magnetic field. *International Journal of Heat and Mass Transfer*, *48*(25–26), 5297–5309. https://doi.org/10.1016/j.ijheatmasstransfer.2005.07.025

Ma, H. B., Wilson, C., Borgmeyer, B., Park, K., Yu, Q., Choi, S. U. S., & Tirumala, M. (2006). Effect of nanofluid on the heat transport capability in an oscillating heat pipe. *Applied Physics Letters*, *88*(14). https://doi.org/10.1063/1.2192971

Nadeem, S., Akhtar, S., & Abbas, N. (2020a). Heat transfer of Maxwell base fluid flow of nanomaterial with MHD over a vertical moving surface. *Alexandria Engineering Journal*, *59*(3), 1847–1856. https://doi.org/10.1016/j.aej.2020.05.008

Nadeem, S., Fuzhang, W., Alharbi, F. M., Sajid, F., Abbas, N., El-Shafay, A. S., & Al-Mubaddel, F. S. (2022b). Numerical computations for Buongiorno nano fluid model on the boundary layer flow of viscoelastic fluid towards a nonlinear stretching sheet. *Alexandria Engineering Journal*, *61*(2), 1769–1778. https://doi.org/10.1016/j.aej.2021.11.013

Norasia, Y., Widodo, B., & Adzkiya, D. (2021). Pergerakan Aliran MHD Ag-AIR Melewati Bola Pejal. *Limits: Journal of Mathematics and Its Applications*, *18*(1), 15. https://doi.org/10.12962/limits.v18i1.7888

Reddy, G. J., Kethireddy, B., Kumar, M., Rani, H. P., & Gorla, R. S. R. (2018). Effect of Prandtl Number for Casson Fluid Flow Over a Vertical Cylinder: Heatline Approach. *International Journal of Applied and Computational Mathematics*, *4*(3). https://doi.org/10.1007/s40819-018-0516-8

Shahzad, F., Jamshed, W., Sajid, T., Shamshuddin, M. D., Safdar, R., Salawu, S. O., Eid, M. R., Hafeez, M. B., & Krawczuk, M. (2022). Electromagnetic Control and Dynamics of Generalized Burgers' Nanoliquid Flow Containing Motile Microorganisms with Cattaneo–Christov Relations: Galerkin Finite Element Mechanism. *Applied Sciences (Switzerland)*, *12*(17). https://doi.org/10.3390/app12178636

Sheikholeslami, M., & Rokni, H. B. (2017). Simulation of nanofluid heat transfer in presence of magnetic field: A review. *International Journal of Heat and Mass Transfer*, *115*, 1203–1233. https://doi.org/10.1016/j.ijheatmasstransfer.2017.08.108

Turkyilmazoglu, M. (2018). Analytical solutions to mixed convection MHD fluid flow induced by a nonlinearly deforming permeable surface. *Communications in Nonlinear Science and Numerical Simulation*, *63*, 373–379. https://doi.org/10.1016/j.cnsns.2018.04.002

Yu, S., Tang, T., Li, J., & Yu, P. (2020). Effect of prandtl number on mixed convective heat transfer from a porous cylinder in the steady flow regime. *Entropy*, *22*(2). https://doi.org/10.3390/e22020184